

on the continental margins, which rapidly prograde to the shelf edge during rising sea levels, leaving large portions of the submerged shelf free to accumulate carbonate. During low sea levels, detritus completely bypasses the shelves, so that clastic sediments almost always accumulate continuously in the continental rises.

If Pacific Ocean accumulation rates represent mainly flux of dissolved carbonate and silica, one might expect a positive correlation between high sea level and carbonate compensation depth (CCD), as suggested by Berger and Winterer (7). However, this correlation is weak at present. Berger (10) noted some similarities between sea level and the CCD for the Cenozoic, but the question of whether sea level and the CCD are coupled remains open because of the difficulty of accurately calculating the Cenozoic history of the CCD.

The suggestion of Davies *et al.* (1) that fluctuations in the input of land-derived material to the deep oceans are related to alternating rates of continental erosion and that these are a consequence of alternating climatic states remains plausible. However, until more detailed estimates are available of the amount of material in the different reservoirs of the geochemical system and of the changing fluxes between the reservoirs, it will not be possible to determine to what extent input of land-derived material to the deep sea is a function of the land/ocean ratio, which is in turn a function of sea level, and to what extent climatic factors influencing continental erosion rates may be involved. We suggest, as have Fisher and Arthur (11), that climate itself is a function of the land/ocean ratio and thus a function of sea level. Thus climate, sea level, and deep-ocean sediment accumulation have a complex dynamic relationship, many details of which remain to be investigated.

THOMAS R. WORSLEY

Department of Geology,
Ohio University,
Athens 45701

THOMAS A. DAVIES

Department of Geology,
Middlebury College,
Middlebury, Vermont 05753

References and Notes

1. T. A. Davies, W. W. Hay, J. R. Southam, T. R. Worsley, *Science* **197**, 53 (1977).
2. T. J. H. van Andel, G. R. Heath, T. C. Moore, *Geol. Soc. Am. Mem.* **143** (1975).
3. *Initial Reports of the Deep Sea Drilling Project* (Government Printing Office, Washington, D.C., 1969-1976), vols. 5-9, 16-21, and 30-32.
4. T. R. Worsley and T. A. Davies, *Mar. Geol.*, in press.
5. P. R. Vail, R. M. Michum, S. Thompson III, in *Seismic Stratigraphy—Applications to Hydrocarbon Exploration*, C. E. Payton, Ed. (American

- Association of Petroleum Geologists, Tulsa, Okla., 1977), pp. 83-97.
6. P. Rona, *Nature (London)* **244**, 25 (1973).
7. W. H. Berger and E. L. Winterer, in *Pelagic Sediments on Land and Under the Sea*, K. J. Hsu and H. C. Jenkyns, Eds. (Blackwell, Oxford, 1974), pp. 11-48.
8. W. W. Hay and J. R. Southam, in *The Fate of Fossil Fuel CO₂ in the Oceans*, N. R. Anderson and A. Malahoff, Eds. (Plenum, New York, 1977), pp. 569-604.
9. H. W. Menard, *Marine Geology of the Pacific* (McGraw-Hill, New York, 1964).
10. W. H. Berger, in *The Fate of Fossil Fuel CO₂ in the Oceans*, N. R. Anderson and A. Malahoff,

Eds. (Plenum, New York, 1977), pp. 505-542.

11. A. G. Fisher and M. L. Arthur, *Soc. Econ. Paleontol. Mineral. Spec. Publ.* **25** (1977), pp. 19-51.
12. The Deep Sea Drilling Project is supported by the National Science Foundation and operated by Scripps Institution of Oceanography with advice from the Joint Oceanographic Institution. We thank P. Woodbury and C. Suchland for their aid in obtaining the data in appropriate format and for their advice. This work was supported by NSF grants OCE-75-04066 and OCE-76-81934.

15 September 1978

Manganese Oxide Tunnel Structures and Their Intergrowths

Abstract. *Natural hollandite and romanechite are widespread barium-containing manganese minerals. High-resolution transmission electron microscopy indicates that intergrowths of the two minerals occur in a coherent manner on the unit-cell level with no apparent ordering of the hollandite and romanechite. Other structures have been imaged that are based on the hollandite and romanechite structures. Electron microscopy holds a key to unraveling the myriad structural complexities of the manganese oxides.*

The oxides of Mn are large in number and complex in character; many of their structures are poorly known. The difficulties associated with distinguishing between them and the extent of intimate mixing that occurs have given rise to the descriptive but intentionally imprecise names of "wad" for the soft oxides and "psilomelane" for the hard, massive, botryoidal variety (1). This report will focus on hollandite, $\sim\text{BaMn}_6\text{O}_{16}$, and mixtures containing hollandite and romanechite, $\sim(\text{Ba},\text{H}_2\text{O})_4\text{Mn}_{10}\text{O}_{20}$ (2).

Hollandite and romanechite, two of the more common psilomelane oxides, occur in sediments, weathered outcrops, the supergene zone of Mn and base metal ore deposits, and metamorphosed Mn deposits. The hollandite structure itself is of interest because it is the form as-

sumed by K, Sr, and Ba feldspars at high pressures, such as occur within the earth's mantle (3).

Our primary method of study has been high-resolution transmission electron microscopy (HRTEM), both by direct structure imaging and by selected area diffraction. These techniques have shown that coherent intergrowths occur between hollandite and romanechite. These intergrowths may account (i) for the reported range in compositions between different hollandites and romanechites and (ii) for the variable and problematical x-ray patterns obtained from romanechite samples (4).

The hollandite and romanechite structures can be placed in a structural classification of Mn oxides that is somewhat analogous to the system developed for rock-forming silicates (5). The $(\text{SiO}_4)^{4-}$ tetrahedron has its counterpart in the $(\text{MnO}_6)^{8-}$ octahedron of MnO_2 minerals. The octahedra share corners and edges to form chain, framework, or sheet structures. The single-chain structure is pyrolusite ($\beta\text{-MnO}_2$), and the double-chain structure is romandellite (MnO_2). Hollandite has a framework structure consisting of double chains of Mn octahedra joined at roughly right angles so as to have a nearly square pattern (2×2) when viewed down the length of chains (Fig. 1a). Romanechite is closely related, with a 3×2 , nearly rectangular arrangement of $(\text{MnO}_6)^{8-}$ chains (Fig. 1b). A variety of large mono- and divalent cations such as K, Na, Ba, Sr, and Pb can then be accommodated within the square or rectangular tunnels thus formed (6).

We studied samples from three localities. We analyzed each sample by (i) x-ray powder diffraction, using a Guinier

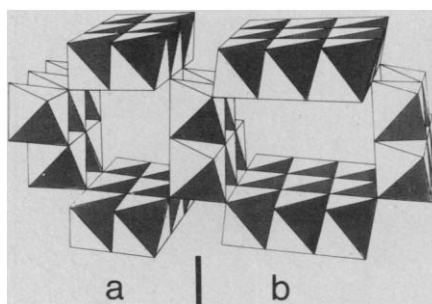


Fig. 1. Schematic of a hollandite-romanechite intergrowth. Each octahedron represents a Mn cation surrounded by six O atoms. (a) Hollandite with its double chains of Mn octahedra. The chains form a square cross section (2×2) when viewed down the tunnel length. (b) Romanechite with its 3×2 rectangular cross section. The double chain is common to both structures and is the basis for unit-cell intergrowths. The tunnels formed in both structures accommodate the large Ba cations or substituting cations.

camera to determine bulk identity, and by (ii) qualitative use of the microprobe to determine cation content. Hollandite from Stuur Njouskes, Sweden (U.S. National Museum sample 127118) was selected because of its purity as shown by its sharp x-ray-diffraction lines. The d spacings (interplanar spacings) from the Guinier pattern were fitted by a least-squares method (7) to give cell parameters of $a = 10.01 (1) \text{ \AA}$, $b = 2.877 (1) \text{ \AA}$, $c = 9.73 (1) \text{ \AA}$, and $\beta = 90^\circ 56 (1)'$. The d spacings and cell parameters correspond closely to those reported for hollandite II, from the same locality (8). Microprobe analysis confirmed Ba and Mn as the major cations, with minor amounts of Pb.

The second sample is from a vein deposit in Tertiary rocks of the Priceless mine, Artillery Mountains, Mohave County, Arizona. A comprehensive x-ray study of Mn oxides from the area (4) had yielded two distinct types of romanechite x-ray patterns, with transitional types between them. Our x-ray data fall in the transitional category, between romanechite I and romanechite II. The chief cations in the sample are Ba and Mn with minor amounts of Sr and K.

The x-ray lines for the third sample, obtained from the Rattlesnake mine in the Luis Lopez district, Socorro County, New Mexico, are diffuse and could be assigned to either hollandite or romanechite spacings. Cations include Ba as well as minor amounts of K.

We used a slightly modified JEOL microscope (JEM 100B) (9). All three samples were prepared by grinding and deposition on a holey carbon film. Some samples from the Priceless and Rattlesnake mines were also ion-thinned perpendicular to their fiber direction.

Viewing down the tunnels, parallel to the b axis of hollandite, we see a roughly square diffraction pattern and a roughly square image for the Stuur Njouskes hollandite (Fig. 2a). The white spots correspond to the tunnels in the double-chain $(\text{MnO}_6)^{8-}$ octahedral framework. There is not sufficient resolution to image the tunnel cations. This image is a good match to a reported computed image of a synthetic material, $\text{BaMgTi}_7\text{O}_{16}$, having the hollandite structure (10). Evidence of at least four types of hollandite with differing a and c parameters and differing

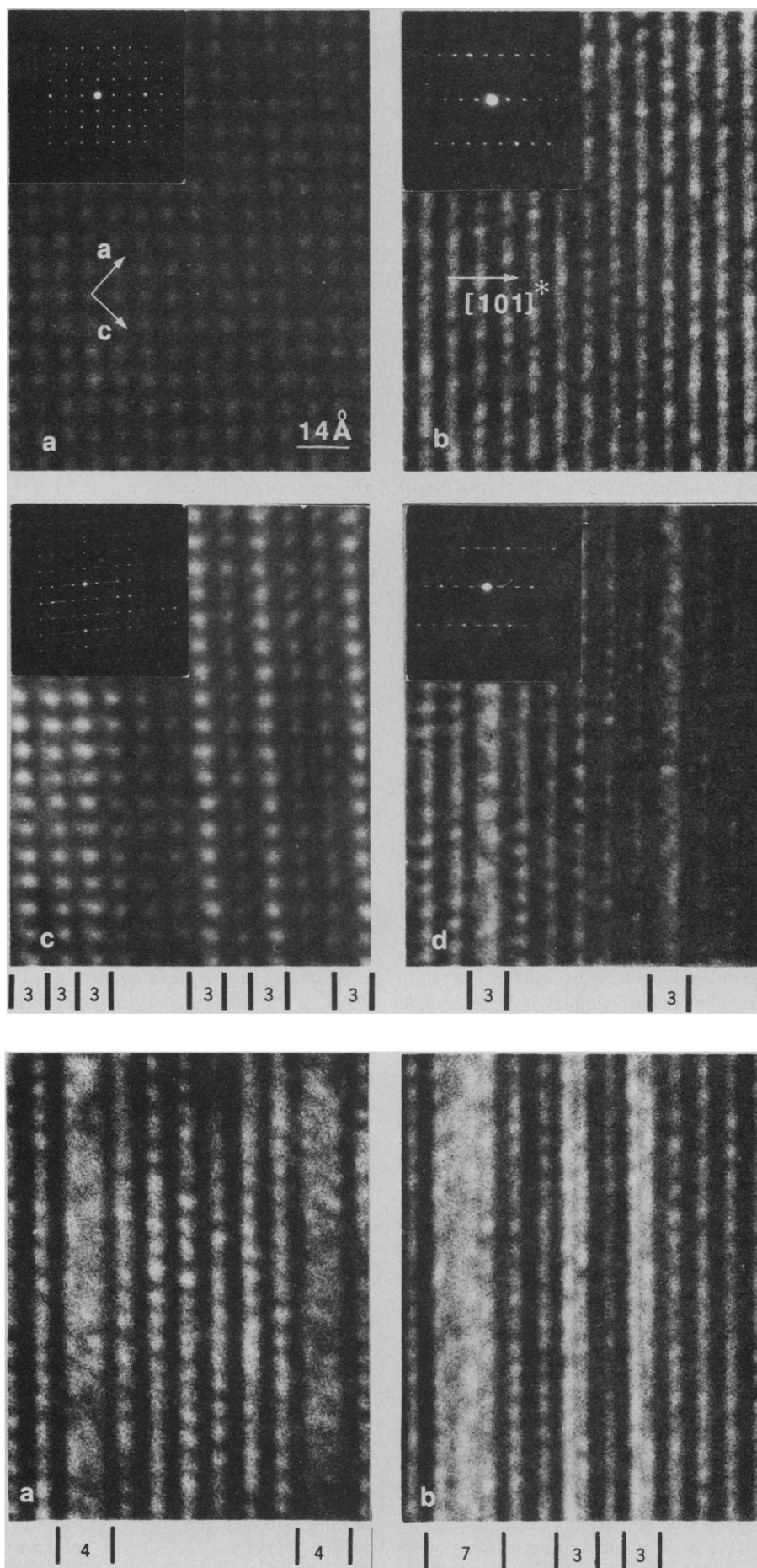


Fig. 2 (top). HRTEM images and electron diffraction patterns of hollandite and hollandite-romanechite mixtures: (a) hollandite viewed down [010]; (b) hollandite viewed so that [101] fringes are evident; (c) hollandite-romanechite mixture viewed down the tunnels, with [3] denoting the wide tunnels corresponding to romanechite; and (d) hollandite-romanechite mixture viewed perpendicular to the chain lengths. The scale is the same for all images in this report.

Fig. 3 (bottom). (a) Two quadruple chains in hollandite. (b) A septuple chain in a hollandite (2×2) -romanechite (3×2) mixture.

β angles can be seen in some crystals in this [010] direction (11).

Any non-[010] pattern that contains (101)* or (10 $\bar{1}$)* gives an image consisting of fringes of roughly 7-Å spacing. One such direction is shown for Swedish hollandite in Fig. 2b. There is no disordering evident; all the electron diffraction patterns and images of Stuur Njouskes hollandite are consistent with its sharp, readily interpreted x-ray pattern.

Viewing along the crystal lengths in the Priceless sample (Fig. 2c), we can see two types of tunnels—square and rectangular, corresponding, respectively, to hollandite and romanechite. Apparently the similarity of the double chains in both hollandite and romanechite permits coherent intergrowths of the two minerals as schematically illustrated in Fig. 1. No evidence of ordering of the intergrowths has been found; the streaking in the diffraction pattern reflects the degree of disorder. The same sorts of features occur in samples from the Rattlesnake mine; intergrowths of romanechite and hollandite are shown along the tunnel lengths in the image (Fig. 2d) of the Rattlesnake sample.

We can obtain some insight into the romanechite structure from the *b* axis images and diffraction patterns. An ambiguity in the literature on the crystal system of romanechite has led to its being reported as both monoclinic (12) and orthorhombic (13). All the romanechite in the romanechite-hollandite mixtures we have thus far observed appears to be monoclinic. Further HRTEM study of romanechite samples is necessary to confirm this deduction as it is possible that the hollandite influences the intergrown romanechite material.

Recently, silicate chains with widths greater than triple have been imaged by HRTEM (14). This is also the case with the octahedral chains of the Mn oxides. We interpret Fig. 3a as containing a quadruple chain associated with hollandite and romanechite, whereas Fig. 3b contains a septuple chain. The structures with greater width have thus far only been seen as isolated chains; corresponding minerals are as yet unknown. However, the crystal structure of todorokite, a Mn oxide found as a major constituent of deep-sea Mn nodules, has not yet been solved. Its structure is thought to be closely related to the hollandite and romanechite structures (4), and so it could possibly be similar to one of the greater-width structures reported here. HRTEM should be of aid in giving a general idea of the todorokite structure.

The known complexity of the Mn oxides derives from the small crystal size—in some cases samples are x-ray amorphous—and the potential for chemical solid solution and structural intergrowths. The present study has demonstrated that intergrowths are common between the hollandite and romanechite structures. Furthermore, HRTEM has been used to show that even wider tunnels can occur as coherent intergrowths. In light of these observations, it is not surprising that the mineralogy of the Mn oxides is complex and has been confusing. It may be expected that HRTEM will be a powerful technique for studying and helping to unravel the structural and chemical complexities of the Mn oxides.

SHIRLEY TURNER

Department of Geology,
Arizona State University,
Tempe 85281

PETER R. BUSECK

Departments of Geology and Chemistry,
Arizona State University

References and Notes

1. Psilomelane has also been used as a mineral name, but the Commission of New Mineral Names voted on 25 August 1969 to make romanechite the name for the specific mineral and psilomelane the general term (M. Fleischer, personal communication).
2. The exact formulas for both hollandite and ro-

manechite are a matter of dispute in the literature. Two suggested formulas are: for hollandite, $(\text{Ba}, \text{K}, \text{Pb})_{2-6}(\text{Mn}, \text{Fe})_{2-2.5}(\text{O}, \text{OH})_{16}(\text{H}_2\text{O})_n$ (7); for romanechite, $(\text{Ba}, \text{H}_2\text{O})_4\text{Mn}_{10}\text{O}_{20}$ (12).

3. A. E. Ringwood, A. F. Reid, A. D. Wadsley, *Acta Crystallogr.* **23**, 1093 (1967); A. F. Reid and A. E. Ringwood, *J. Solid State Chem.* **1**, 6 (1968).
4. M. M. Mouat, *Am. Mineral.* **47**, 744 (1962).
5. R. G. Burns and V. M. Burns, in *Proceedings of an International Symposium on Manganese*, A. Kozawa and R. J. Brodd, Eds. (Electrochemical Society, Princeton, N.J., 1975), pp. 306–327.
6. This cation variability results in a family of minerals with the hollandite structure: Pb-coronadite, K-cryptomelane, and Na-manjiroite.
7. D. E. Appleman and H. T. Evans, *U.S. Geological Survey Computer Contribution No. 20* (National Technical Information Service, Springfield, Va., 1973).
8. A. Byström and A. M. Byström, *Acta Crystallogr.* **3**, 146 (1950).
9. P. R. Buseck and S. Iijima, *Am. Mineral.* **59**, 1 (1974).
10. L. A. Bursill and A. R. Wilson, *Acta Crystallogr. Sect. A* **33**, 672 (1977).
11. S. Turner and P. R. Buseck, in preparation.
12. A. D. Wadsley, *Acta Crystallogr.* **6**, 433 (1953).
13. B. Mukherjee, *Mineral. Mag.* **35**, 643 (1965).
14. J. L. Hutchison, D. A. Jefferson, L. G. Mallinson, J. M. Thomas, *Mater. Res. Bull.* **11**, 1557 (1976); D. R. Veblen, P. R. Buseck, C. W. Burnham, *Science* **198**, 359 (1977); D. A. Jefferson, L. G. Mallinson, J. L. Hutchison, J. M. Thomas, *Contrib. Mineral. Petrol.* **66**, 1 (1978); M. Czank and P. R. Buseck, *Z. Krist.*, in press.
15. We thank J. M. Cowley, I. Mackinnon, and D. Veblen for valuable discussion; J. Hunt for microprobe work; and J. Wheatley for assistance in the electron microscope laboratory in the Center for Solid State Science at Arizona State University. We thank D. J. Fischer for recommending and the Rocky Mountain Mineralogical Society for awarding S.T. a scholarship. The research was supported in part by grant EAR 77-00128 from the National Science Foundation Earth Sciences Division.

2 August 1978; revised 2 October 1978

Biological Bulldozers and the Evolution of Marine Benthic Communities

Abstract. During the Phanerozoic, the diversity of immobile suspension feeders living on the surface of soft substrata (ISOSS) declined significantly. Immobile taxa on hard surfaces and mobile taxa diversified. Extinction rates of ISOSS were significantly greater than in other benthos. These changes in the structure of benthic communities are attributed to increased biological disturbance of the sediment (bioturbation) by diversifying deposit feeders.

Most marine fossils are preserved in fine-grained, originally soft sediments. In the Paleozoic these habitats were dominated by immobile suspension feeders (1, 2): articulate brachiopods, dendroid graptolites, tabulate and rugose corals, bryozoa, cystoids, blastoids, and Archecocyatha (the only known extinct phylum). Physically equivalent environments are now occupied primarily by deposit feeders (3, 4), for example, protobranch bivalves, irregular echinoids, and certain crustacea, holothurians, and annelids. I suggest that newly evolved deposit feeders and other sediment-disturbing taxa displaced the immobile suspension feeders on soft substrata (ISOSS).

Deposit feeders "mine" organic particles from mud or sand (5, 6), whereas

suspension feeders filter food particles from the water column. In Recent marine communities, deposit feeders may exclude suspension feeders by bioturbation (7, 8). This includes suspending sediment or feces that foul biological filters, fluidizing mud substrata (9), accidental ingestion (10), as well as bulldozing; overturning or burial of ISOSS. The effects of bulldozing will be greatest when the deposit feeders are much larger than the ISOSS; juvenile ISOSS will be especially susceptible (3, 6). If the ISOSS cannot complete their life cycles before the sediment is disturbed, they are unlikely to persist. Scavengers and predators may also act as bulldozers (3, 11, 12).

Modern bulldozers—holothurians, irregular echinoids (13), malacostracan